Transactions on Engineering Sciences vol 13, © 1996 WIT Press, www.witpress.com, ISSN 1743-3533

Fatigue crack growth mechanism of MMC at room and higher temperatures

T. Tanaka,[a] H. Nakayama,[b] Y. Kobayashi[c]
[a]*Department of Mechanical Engineering, Faculty of Science and Engineering, Ritsumeikan University, Noji-cho, Kusatsu, 525-77, Japan*
[b]*Department of School Juridical Person, Osaka Sangyo University, Nakagaito, Daito, 574, Japan*
[c]*Graduate student, Ritsumeikan University, Noji-cho, Kusatsu, 525-77, Japan*

Abstract

In order to clarify the fatigue failure mechanism of an alumina short fiber reinforced aluminum alloy (hereafter, MMC for brevity), a series of fatigue strength and fatigue crack growth tests was carried out at room and elevated temperatures. Aluminum alloy A6061 was used as a reference material. Results of fatigue strength tests showed that the fatigue strength of the MMC was superior to that of A6061 alloy in long life region and at higher temperature. Similar trend was also found from the results of fatigue crack growth tests, that is, the MMC showed higher threshold level and relatively lower dependence of the crack growth rate on the temperature when compared with the case of A6061 alloy. Moreover, it was found that the fatigue crack growth rate of the MMC was governed by both K_{max} and ΔK_{eff} and its temperature dependence was expressed in terms of the 0.2% proof stress, Young's modulus and a parameter relating to the crack closure at each temperature.

1 Introduction

Alumina short fiber reinforced aluminum alloy (MMC) is a metal matrix composite with several advantages such as weight-saving, high intensity to density and excellent high temperature strength, which is developed for applications to automobile engine parts.[1-6] But the fatigue properties of this composite are almost unknown at present because of the scarcity of strength data.

In this study, fully reversed push-pull fatigue strength tests were first carried out on the MMC at several temperatures up to 280℃ in order to examine the temperature dependence of the fatigue strength. Then a series of fatigue crack growth tests was carried out at room temperature, 170℃ and 280℃, under pulsating tensile load conditions with several stress ratios from 0.1 to 0.7. The results were discussed in comparison with those of A6061 alloy.

Attempts were made to find the suitable fracture mechanics parameters governing the fatigue crack growth rate of the MMC under different stress ratios and at different temperatures.

2 Materials and experimental procedures

The MMC used in this study consists of aluminum alloy A6061 and alumina short fibers with the average diameter of 3μm and the average length of 100μm. The volume fraction of alumina short fiber is in the range from 34.5 to 43.1%. This composite was produced by pressure-casting method and as-casted composite was supplied to the experiments, in which aluminum alloy matrix was in as-casted condition and alumina short fibers were distributed almost uniformly in random directions. Table 1 shows mechanical properties of the MMC and A6061-T6 alloy used as reference material at respective temperature levels. Ultimate tensile strength of the MMC is lower than that of A6061 alloy at each temperature, and tensile strengths and Young's moduli of both materials decrease with the increase in the temperature.

Fully reversed push-pull fatigue strength tests were carried out at room temperature, 100℃, 170℃, 220℃ and 280℃ at a loading frequency of 20Hz. Fatigue crack growth tests were carried out under pulsating tensile load conditions at room temperature, 170℃ and 280℃. At room temperature and

Table 1: Mechanical properties.

Material	Temperature T (℃)	0.2% proof stress $\sigma_{0.2}$ (MPa)	Ultimate tensile stress σ_B (MPa)	Elongation δ (%)	Young's modulus E (GPa)
MMC	R.T.	156	222	2	103.6
	170	136	204	–	100.2
	280	115	118	–	92.1
A6061-T6	R.T.	268	283	19	72.8
	170	–	242	–	70.0
	280	–	152	–	63.4

170°C, the stress ratios were R=0.1, 0.3, 0.5 and 0.7, but at 280°C the highest stress ratio was 0.5. The loading frequency for fatigue crack growth tests was 20 Hz.

3 Results and discussion

Figure 1 shows the results of fatigue strength tests plotted on S–N diagram. It is observed that the fatigue strengths of both the MMC and the aluminum alloy base metal decrease with the increase in the temperature. In the range from room temperature to 170°C, the fatigue strength of the MMC is lower than that of A6061 alloy in the whole stress cycles range, but such a superiority of A6061 in fatigue strength to the MMC is reversed at about 10^6 cycles at 220°C, and in the whole stress cycles range at 280°C.

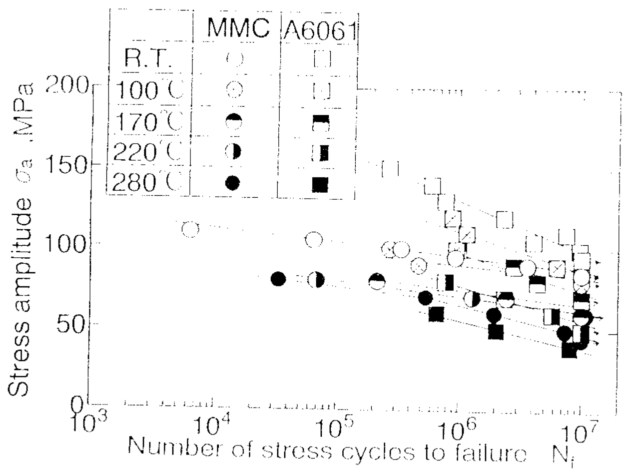

Figure 1: S–N curves.

Figures 2 and 3 show the fatigue crack growth rate curves for both materials. It is clear, from both figures, that the fatigue crack growth rates of both materials can be governed neither by K_{max} nor by ΔK. Figure 4 is a schematical reproduction of Fig.2, in which the fatigue crack growth rates of both materials at all test temperatures are shown for each stress ratio. Figures 4 (a) and (b) indicate that the temperature dependence of the fatigue crack growth rate of the MMC is very small in comparison with that of A6061 alloy, and that the crack growth resistance of the MMC is superior to that of A6061 alloy in the lower crack growth rate region including the threshold. However, these advantages of the MMC are gradually diminished for the higher stress ratios of R=0.5 and 0.7 as observed in Figs.4 (c) and (d).

Figure 5 shows the relationship between the fatigue crack growth rate and the effective stress intensity factor range ΔK_{eff} for the MMC, where ΔK_{eff} at room temperature was measured during the tests, but that at elevated

Transactions on Engineering Sciences vol 13, © 1996 WIT Press, www.witpress.com, ISSN 1743-3533

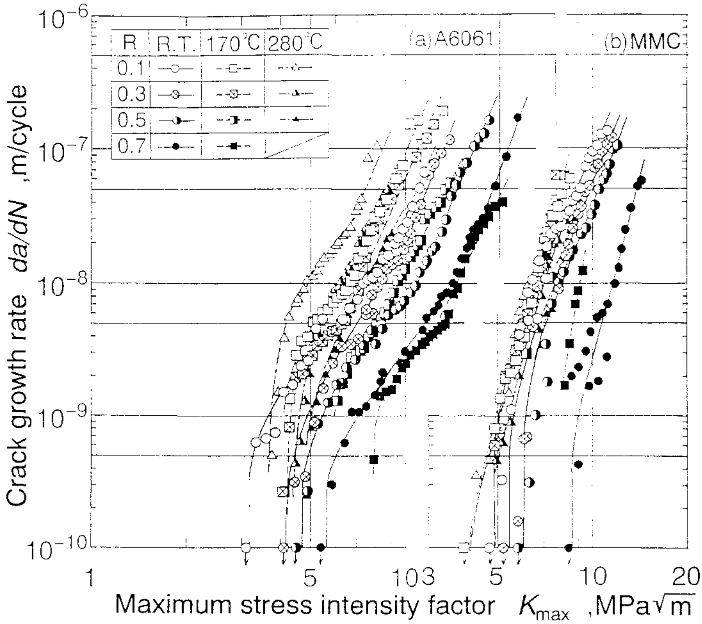

Figure 2: $da/dN-K_{max}$ curves for (a) A6061 and (b) MMC.

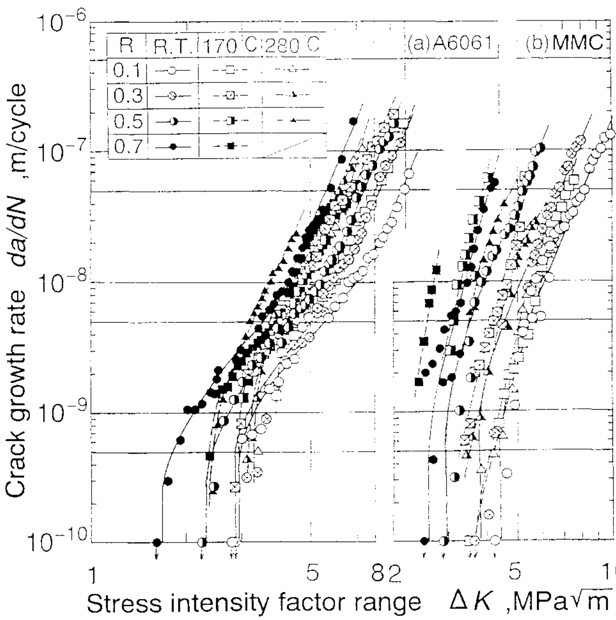

Figure 3: $da/dN-\Delta K$ curves for (a) A6061 and (b) MMC.

Transactions on Engineering Sciences vol 13, © 1996 WIT Press, www.witpress.com, ISSN 1743-3533

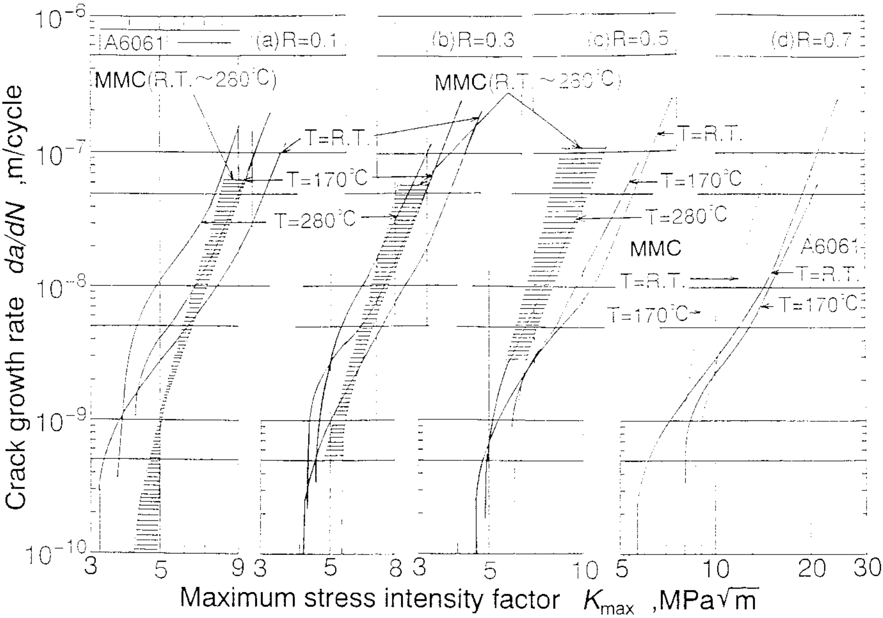

Figure 4: da/dN–K_{max} curves at each stress ratio for A6061 and MMC.

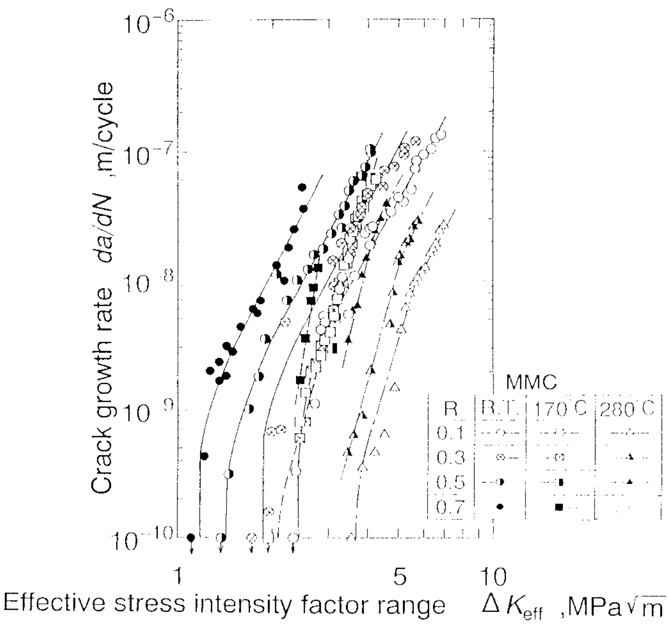

Figure 5: $da/dN-\Delta K_{eff}$ curves for MMC.

Transactions on Engineering Sciences vol 13, © 1996 WIT Press, www.witpress.com, ISSN 1743-3533

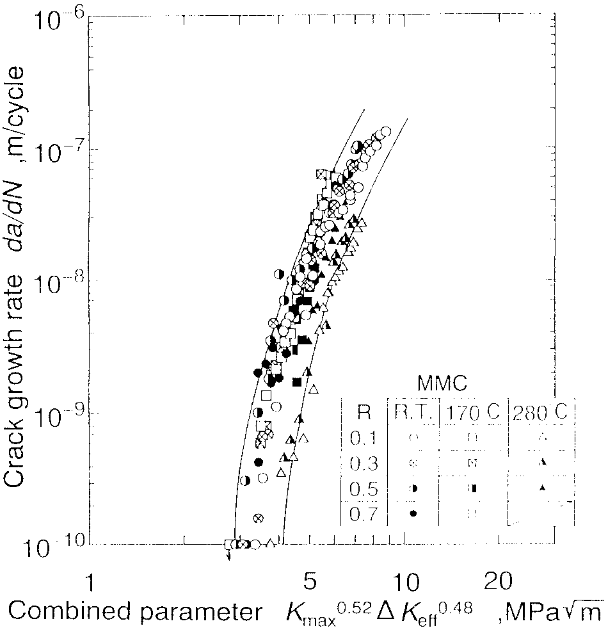

Figure 6: $da/dN - K_{max}{}^{\alpha} \Delta K_{eff}{}^{(1-\alpha)}$ curves for MMC.

temperatures is estimated value based on several assumptions.[8] It is seen that the fatigue crack growth rate of the MMC is not governed by ΔK_{eff} even at room temperature.

Figure 6 shows the relationship between the fatigue crack growth rate and combined fracture mechanics parameter defined as $K_{max}{}^{\alpha} \Delta K_{eff}{}^{(1-\alpha)}$, where α is equal to 0.52 in this study.[7] It is observed that the fatigue crack growth rates at room temperature and at 170℃ are governed by this combined parameter and the difference in crack growth rate due to the testing temperature diminishes. But, the data at 280℃ are located at right hand side of the scatter band.

Figure 7 illustrates the effect of the stress ratio R on ΔK or ΔK_{eff} which gives the same crack growth rate on stage II_b of crack growth curve at room and elevated temperatures (RT and HT). Although ΔK_{RT} is higher than ΔK_{HT} in the lower stress ratio (R_a), such a situation is reversed in the higher stress ratio (R_c), because $\Delta K_{eff,RT}$ is lower than $\Delta K_{eff,HT}$. This is the point to be considered to determine which parameter governs the fatigue crack growth rates in the wide range of temperature.[8] If it is assumed that the crack tip opening displacement $\Delta CTOD$ at room temperature is equal to that at higher temperatures at R=0 for the same crack growth rate, then we obtain the equation of $\Delta K_{RT,R=0} / \sqrt{(E\sigma_{0.2})_{RT}} = \Delta K_{HT,R=0} / \sqrt{(E\sigma_{0.2})_{HT}}$ from the equation of $\Delta CTOD = \Delta K^2/(E\sigma_{0.2})$, and have a parameter $U_R(1-R)K_{max} / \sqrt{(E\sigma_{0.2})}U_{R=0}$, where, $\Delta K_{R=0} = \Delta K_{eff} / U_{R=0} = U_R \Delta K / U_{R=0} = U_R(1-R)K_{max} / U_{R=0}$. In fact, this was consistent with the experimental results. By using this parameter, Fig.8 is

Transactions on Engineering Sciences vol 13, © 1996 WIT Press, www.witpress.com, ISSN 1743-3533

reproduced from Fig.6 and it is found that the crack growth rate curves in all test conditions are well controlled by the parameter $(U_R(1-R) \, / \, U_{R=0.1})^{(1-\alpha)}K_{max} \, / \, \sqrt{(E\sigma_{0.2})}$ which was calculated by using $U_{R=0.1}$ instead of $U_{R=0}$.

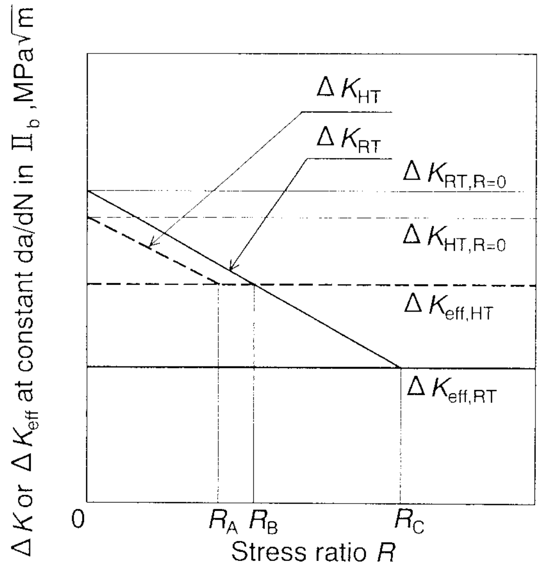

Figure 7: Schematic illustration for relationships between ΔK, ΔK_{eff} and R.

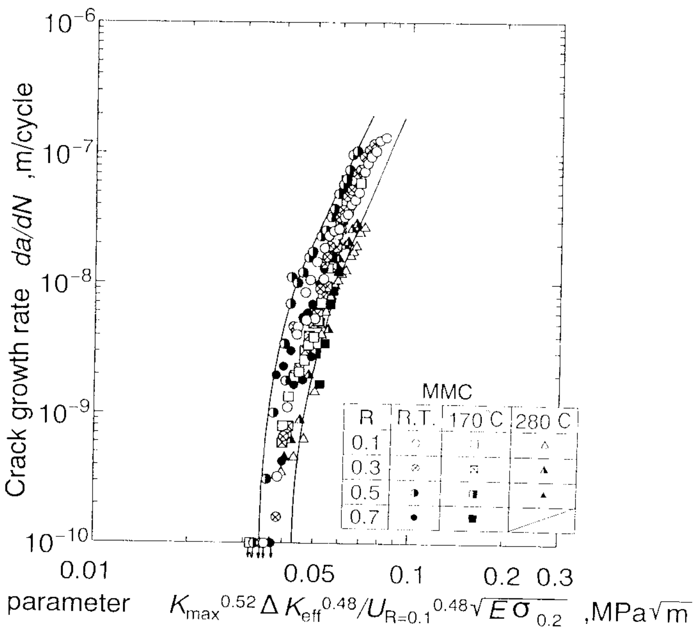

Figure 8: $da/dN-K_{max}{}^{\alpha}\Delta K_{eff}{}^{(1-\alpha)}/(U_{R=0.1}{}^{(1-\alpha)}\sqrt{(E\sigma_{0.2})})$ curves for MMC.

4 CONCLUSION

It was found that the fatigue strength of the MMC was higher than that of A6061 alloy in the long life region at high temperatures above 170℃ and that the crack growth resistance of the MMC was superior to that of A6061 alloy for lower stress ratio in the low crack growth rate region. Moreover, the temperature dependence of the crack growth rate of the MMC was small when compared with that of A6061 alloy for lower stress ratio, but this advantage was gradually diminished for higher stress ratio. It was revealed that the crack growth rate curves of the MMC was governed by the combined prameter $K_{max}{}^{\alpha}\Delta K_{eff}{}^{(1-\alpha)} / (U_{R=0}{}^{(1-\alpha)}\sqrt{(E\sigma_{0.2})})$ in all test conditions.

REFERENCES

1. Donomoto, T. Ceramic fiber alloy for high performance diesel pistons , *Journal of the Society of Automotive Engineers of Japan*, 1983, **37**, 884–889

2. Ohori, K., Watanabe H. & Takeuchi Y. Silicon carbide whisker reinforced aluminium composite–fabrication and properties, *Materials Science and Technology*, 1987, **3**, 57–60

3. Divecha, A.P., Fishman, S.G. & Karmarkar S.D. Silicon carbide reinforced aluminum – a formable composite, *Journal of Metals*, 1981, **9**, 12–17

4. Dinwoodie, J. Automotive applications for MMC's based on short staple alumina fibers, *SAE Journal*, 1988, **2**, 269–279

5. Chi, F.K., Austen, R.D., Maier, R.D. & Krucek T.W. Short ceramic fiber reinforced aluminum alloy, *SAE Journal*, 1988, **2**, 280–285

6. Hayashi, N., Ban, K. & Sakurai H. Development of fiber reinforced aluminum connecting rod, *Bulletin of Japan Institute of Metals*, 1986, **25**, 565–567

7. Tanaka, T., Nakayama, H., Yamamoto, S. & Kobayashi, Y. Fatigue crack growth behavior of alumina short fiber reinforced aluminum alloy at room temperature, *Journal the Society of Materials Science, Japan*, 1995, **44**, 945–952

8. Tanaka, T., Nakayama, H., Yamamoto, S. & Kobayashi, Y. Fatigue crack growth behavior of alumina short fiber reinforced aluminum alloy at room and higher temperatures, *Journal the Society of Materials Science, Japan*, 1995, **45**, 64–71